

Drag

Drag Bookkeeping

Drag may be divided into components in several ways:

To highlight the change in drag with lift:

$$\text{Drag} = \text{Zero-Lift Drag} + \text{Lift-Dependent Drag} + \text{Compressibility Drag}$$

To emphasize the physical origins of the drag components:

$$\text{Drag} = \text{Skin Friction Drag} + \text{Viscous Pressure Drag} + \text{Inviscid (Vortex) Drag} + \text{Wave Drag}$$

The latter decomposition is stressed in these notes. There is sometimes some confusion in the terminology since several effects contribute to each of these terms. The definitions used here are as follows:

Compressibility drag is the increment in drag associated with increases in Mach number from some reference condition. Generally, **the reference condition is taken to be $M = 0.5$** since the effects of compressibility are known to be small here at typical conditions. Thus, compressibility drag contains a component at zero-lift and a lift-dependent component but includes only the increments due to Mach number (C_L and Re are assumed to be constant.)

Zero-lift drag is the drag at $M=0.5$ and $C_L = 0$. It consists of several components, discussed on the following pages. **These include viscous skin friction, vortex drag due to twist, added drag due to fuselage upsweep, control surface gaps, nacelle base drag, and miscellaneous items.**

The *Lift-Dependent drag*, sometimes called induced drag, includes the usual lift-dependent vortex drag together with lift-dependent components of skin friction and pressure drag.

For the second method:

Skin Friction drag arises from the shearing stresses at the surface of a body due to viscosity. It accounts for most of the drag of a transport aircraft in cruise.

Viscous pressure drag also is produced by viscous effects, but not so directly. The pressure distribution is modified by the presence of a boundary layer.

Although in 2-D inviscid flow the pressures on forward and aft surfaces balance so that no drag is produced, the effect of the boundary layer leads to an imperfect canceling of these pressures so some additional drag is created.

Inviscid or vortex drag is produced by the trailing vortex wake of a three-dimensional lifting system.

Wave drag is produced by the presence of shock waves at transonic and supersonic speeds. It is the result of both direct shock losses and the influence of shock waves on the boundary layer. The wave drag is often decomposed into a portion related to lift and a portion related to thickness or volume.

In these notes, a somewhat more detailed drag breakdown is used. The total drag is expressed as the sum of the following components:

Drag =
Non-lifting skin friction and pressure drag
+ Fuselage Upsweep Drag
+ Control Surface Gap Drag
+ Nacelle Base Drag
+ Miscellaneous Items

+ Vortex Drag
+ Lift-Dependent Viscous Drag
+ Wave Drag (Lift-Dependent and Volume-Dependent)

The first five of these items do not change as the lift changes and are taken together as the parasite drag. This is not quite the same as the drag at zero lift because the zero lift drag may include vortex drag when the wing is twisted. Another drag item that is sometimes considered separately is trim drag, the drag increment associated with the required tail load to trim the aircraft in pitch. Here we consider trim drag in the discussion of vortex drag of the lifting system.

Nomenclature

The drag is often expressed in dimensionless form:

$$C_D = D/qS_{ref}$$

where S_{ref} is the reference area. The reference area is not so clear when the wing is not a simple tapered planform, but for the purposes of this class, it is taken to be the projected area of the equivalent trapezoidal wing planform.

The parasite drag is often written in terms of the equivalent flat plate drag area, f :

$$f = C_{D_p} S_{ref} = \text{Parasite Drag}/q$$

Drag Components

Subsequent sections deal in some detail with each of the components of the aircraft drag. The drag associated with compressibility is treated in the following chapter.

The parasite drag components include:

- **Non-lifting skin friction and viscous pressure drag**
- **Fuselage Upsweep Drag**
- **Control Surface Gap Drag**
- **Nacelle Base Drag**
- **Miscellaneous Items**

The parasite drag of a typical airplane in the cruise configuration consists primarily of the skin friction, roughness, and pressure drag of the major components. There is usually some additional parasite drag due to such things as fuselage upsweep, control surface gaps, base areas, and other extraneous items. Since most of the elements that make up the total parasite drag are dependent on Reynolds number and since some are dependent on Mach number, it is necessary to specify the conditions under which the parasite drag is to be evaluated. In the method of these notes, the conditions selected are the Mach number and the Reynolds number corresponding to the flight condition of interest.

The basic parasite drag area for airfoil and body shapes can be computed from the following expression:

$$f = k c_f S_{wet}$$

where the skin friction coefficient, c_f , which is based on the exposed wetted area includes the effects of roughness, and the form factor, k , accounts for the effects of both superelevations and pressure drag. S_{wet} is the total wetted area of the body or surface.

Computation of the overall parasite drag requires that we compute the drag area of each of the major components (fuselage, wing, nacelles and pylons, and tail surfaces) and then evaluate the additional parasite drag components described above.

We thus write:

$$C_{D_p} = S k_i c_{f_i} S_{wet_i} / S_{ref} + C_{D_{upsweep}} + C_{D_{gap}} + C_{D_{nac_base}} + C_{D_{misc}}$$

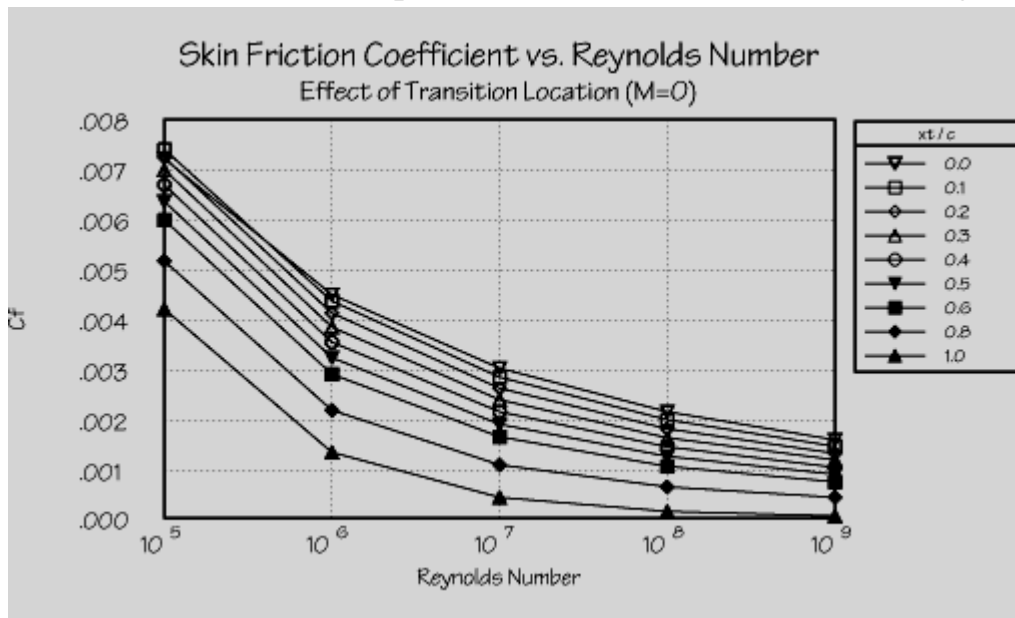
where the first term includes skin friction, and pressure drag at zero lift of the major

components. c_{f_i} is the average skin friction coefficient for a rough plate with transition at flight Reynolds number. Equivalent roughness is determined from flight test data.

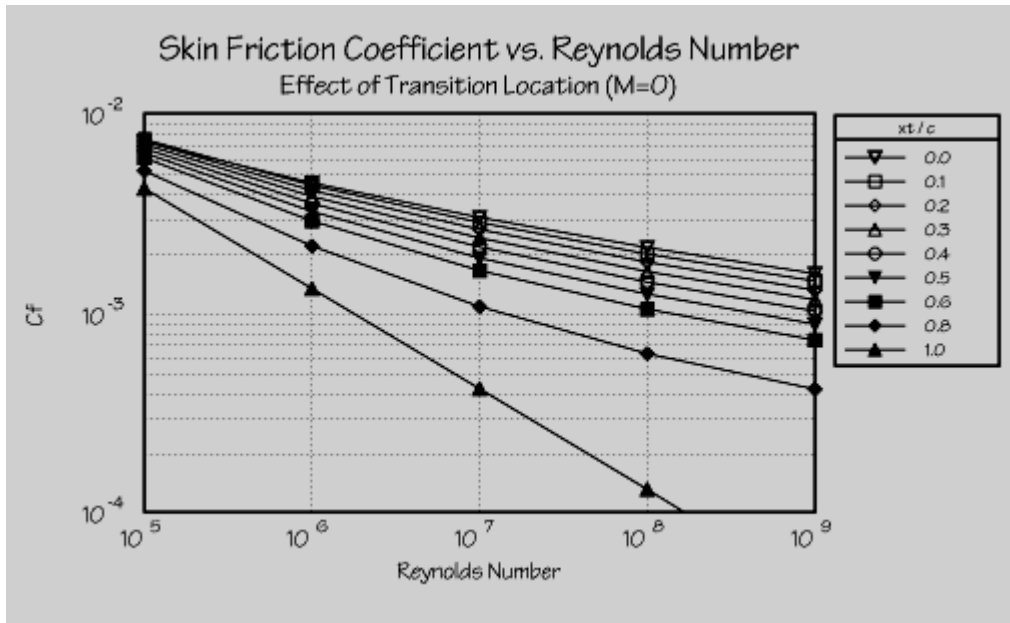
These computations are divided into evaluation of the following terms:

Skin friction coefficient, c_f

The skin friction coefficients are sometimes based on experimental data for flat plates with various amounts of roughness. In the present method, experimental results for turbulent flat plates are fit and combined with basic laminar flow boundary layer theory to produce the data in the figure below. The data apply to insulated flat plates with transition from laminar to turbulent flow specified as a fraction of the chord length ($x_t/c = 0$ represents fully turbulent flow.) The data are total coefficients; that is, they are average values for the total wetted area of a component based on the characteristic length of the component.



When the skin friction is plotted on a log-log scale the curves are nearly straight lines, but the actual variation of c_f is more pronounced at lower Reynolds numbers.

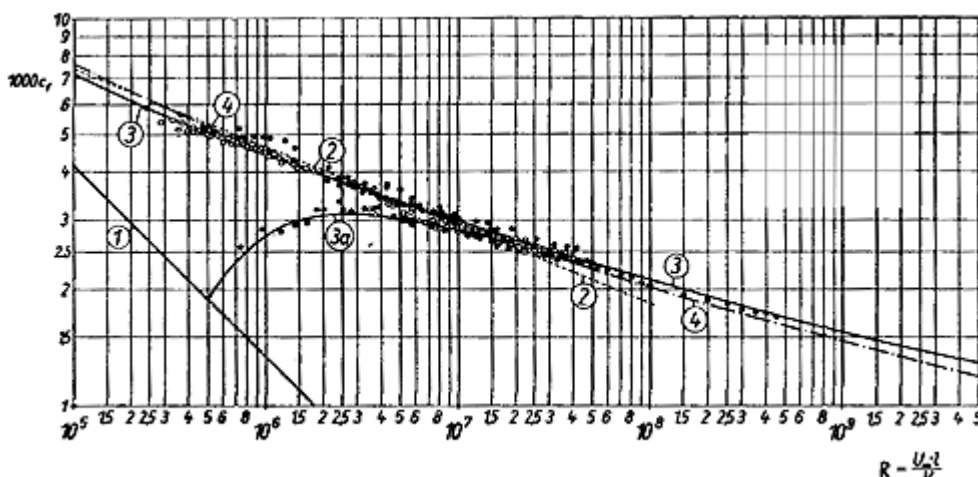


For fully turbulent plates, the skin friction coefficient may be approximated by one of several formula that represent simple fits to the experimentally-derived curves shown in the above figure. For incompressible flow:

$$c_f = \frac{.455}{(\log Re)^{2.58}} \quad \text{or} \quad c_f = \frac{0.074}{Re^{0.2}}$$

The logarithmic fit by von Karman seems to be a better match over a larger range of Reynolds number, but the power law fit is often more convenient. (Note that the log in the above expression is log base 10, not the natural log, denoted “ \ln ” here.)

In the computation of Reynolds number, $Re = \rho VL/\mu$, the characteristic length, L , for a body (fuselage, nacelle) is the overall length, and for the aerodynamic surfaces (wing, tail, pylon) it is usually the *exposed* mean aerodynamic chord. The values of density (ρ), velocity (V), and viscosity (μ) are obtained from standard atmospheric conditions at the point of interest. For our purposes we often use the initial cruise conditions. Atmospheric data may be computed in the atmospheric calculator included here.



Experimental measurements of skin friction coefficient compared with curve fits. Note scatter and transition between laminar and turbulent flow.

Roughness

It is, for all practical purposes, impossible to explicitly define the incremental drags for all of the protruding rivets, the steps, the gaps, and bulges in the skin; the leakage due to pressurization; etc. Instead, in the method of these notes, an overall markup is applied to the skin friction drag to account for drag increments associated with roughness resulting from typical construction procedures. Values of the roughness markup factor have been determined for several subsonic jet transports by matching the flight-test parasite drag with that calculated by the method described in these notes. The values so determined tend to be larger for smaller airplanes, but a 6%-9% increase above the smooth flat values shown in the figure is reasonable for initial design studies. Carefully-built laminar flow, composite aircraft may achieve a lower drag associated with roughness, perhaps as low as 2-3%.

The drag assigned to roughness also implicitly accounts for all other sources of drag at zero lift that are not explicitly included. This category includes interference drag, some trim drag, drag due to unaligned control surfaces, drag due to landing gear door gaps, and any excess drag of the individual surfaces. Consequently the use of the present method implies the same degree of proficiency in design as that of the airplanes from which the roughness drag correlation was obtained.

Effect of Mach Number

The friction coefficient is affected by Mach number as well. The figure below shows that this effect is small at subsonic speeds, but becomes appreciable for supersonic aircraft. For this course, the effect may be approximated from the plot below, but a computational approach is described by Sommer and Short in NACA TN 3391 in 1955. The idea is that aerodynamic heating modifies the fluid properties. If one assumes a wall recovery factor (the ratio of the actual stagnation temperature to the adiabatic stagnation temperature) of 0.89 (a reasonable estimate), and fully-turbulent flow, the wall temperature may be estimated from:

$$T_w/T_\infty = 1 + 0.178M_\infty^2$$

An effective incompressible temperature ratio is defined:

$$T'/T_\infty = 1 + 0.035 M_\infty^2 + 0.45(T_w/T_\infty - 1)$$

leading to an effective Reynolds number:

$$R'/R_\infty = [(T_\infty + 216)/(T' + 216)](T_\infty/T')^{1.5}$$

when the viscosity ratio is given by the Sutherland formula (with T in units of °R):
The compressible skin friction coefficient is then given by:

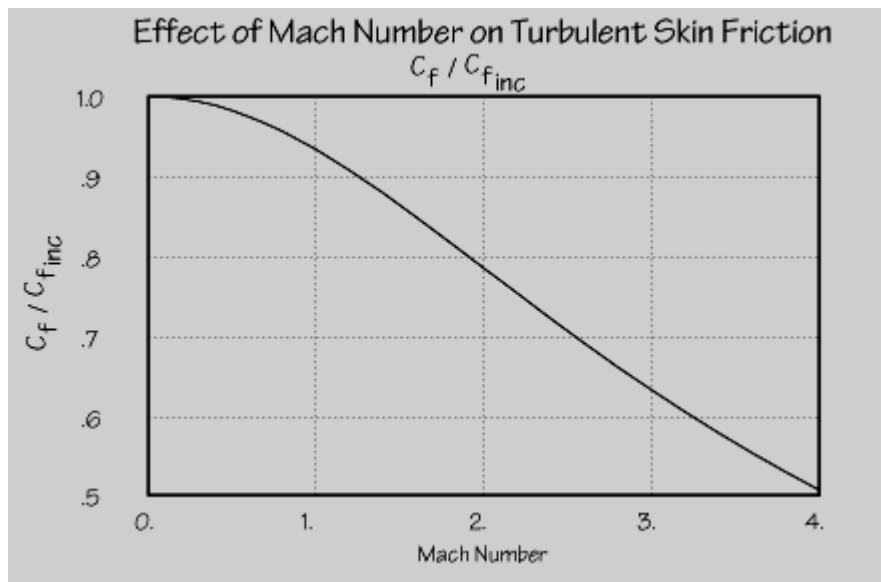
$$c_f = (T_\infty/T') c'_{f_{inc}}$$

where $c'_{f_{inc}}$ is the incompressible skin friction coefficient, computed at the Reynolds number R' .

Finally, the ratio of compressible C_f to incompressible C_f at the same Reynolds number is:

$$c_f/c_{f_{inc}} = (T_\infty/T') (R_\infty/R')^{0.2}$$

The net result is shown in the plot below.



Note that the difference in C_f between Mach 0 and Mach 0.5 is about 3%.

Form factor, k

The parasite drag associated with skin friction and pressure drag is determined by incrementing the flat plate results by a factor, k, to account for pressure drag and the higher-than-freestream surface velocities:

$$f = k c_f S_{wet}$$

The principal cause of increased drag is the increased surface velocity (supervelocity) due to thickness. For a given airfoil we can compute the maximum increase in velocity. This can also be done for a range of airfoil thickness ratios, wing sweeps, and Mach numbers to

determine the form of variation with these parameters. After that one must still resort to experimental data to correlate the actual drag increment associated with skin friction and pressure drag. Such a variation is shown in the figure below at a Mach number of 0.5 for a family of airfoils similar to those used on commercial transports.

Form Factor for Lifting Surfaces

The principal cause of increased drag is the increased surface velocity (supervelocity) due to thickness. This may be computed as follows for wing-like surfaces. Consider an infinite swept wing with a perturbation due to thickness of:

$\Delta U_n(x)$ and define $\Delta U' = \Delta U_n / U_\infty$. The surface velocity is then:

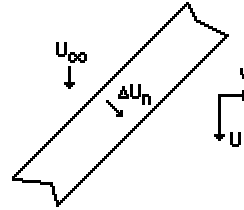
$$U = U_\infty + \Delta U_n \cos \Lambda \quad \text{and} \quad V = \Delta U_n \sin \Lambda$$

and resultant is:

$$U_{tot}^2 = U^2 + V^2 = U_\infty^2 + \Delta U_n^2 + 2 U_\infty \Delta U_n \cos \Lambda$$

The skin friction drag coefficient is given by:

$$\begin{aligned} C_D &= C_f U_{tot}^2 / U_\infty^2 U / U_{tot} S_{wetted} / S \\ &= C_f U U_{tot} / U_\infty^2 S_{wetted} / S \\ &= C_f (U_\infty + \Delta U_n \cos \Lambda) (U_\infty^2 + \Delta U_n^2 + 2 U_\infty \Delta U_n \cos \Lambda)^{0.5} / U_\infty^2 S_{wetted} / S \\ &= C_f (1 + \Delta U' \cos \Lambda) (1 + \Delta U'^2 + 2 \Delta U' \cos \Lambda)^{0.5} S_{wetted} / S \\ &= C_f [(1 + 2 \Delta U' \cos \Lambda + \Delta U'^2 \cos^2 \Lambda) (1 + \Delta U'^2 + 2 \Delta U' \cos \Lambda)]^{0.5} S_{wetted} / S \\ &= C_f [1 + \Delta U'^2 + 2 \Delta U' \cos \Lambda + 2 \Delta U' \cos \Lambda + 4 \Delta U'^2 \cos^2 \Lambda + \Delta U'^2 \cos^2 \Lambda + \text{HOTs}]^{0.5} S_{wetted} / S \\ &= C_f [1 + 4 \Delta U' \cos \Lambda + \Delta U'^2 (1 + 5 \cos^2 \Lambda) + \text{HOTs}]^{0.5} S_{wetted} / S \\ &\approx C_f [1 + 2 \Delta U' \cos \Lambda + \Delta U'^2 (1 + 5 \cos^2 \Lambda) / 2] S_{wetted} / S \end{aligned}$$



Ignoring the reduction in c_f due to Reynolds number and Mach number changes associated with the increased local velocity, because this cannot be computed at all well and because c_f varies weakly with these:

$$k = 1 + 2 \Delta U' \cos \Lambda + \Delta U'^2 (1 + 5 \cos^2 \Lambda) / 2$$

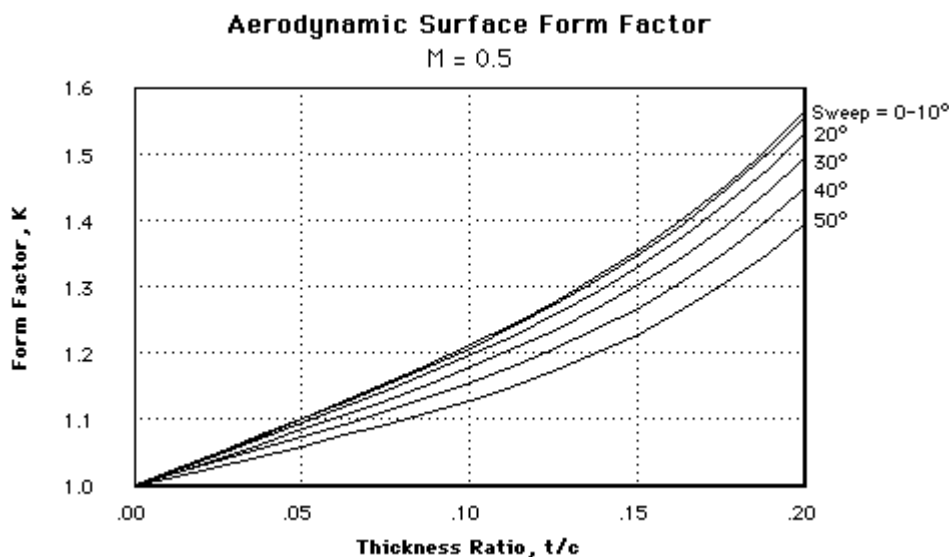
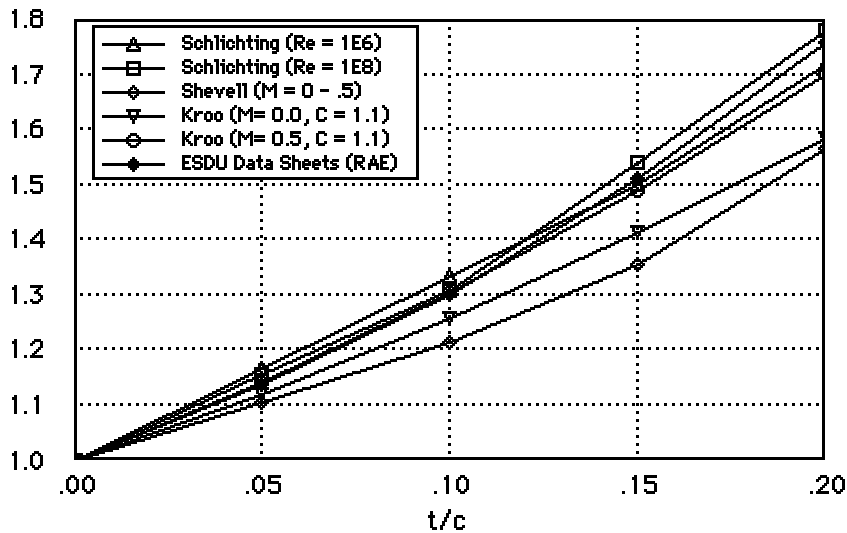
Now in incompressible flow, $\Delta U' = C (t/c)$, even for large t/c (with t/c measured in the normal direction). In 2-D subsonic flow:

$$U' = C (t/c) \cos \Lambda (1 - M_\infty^2)^{-0.5} = C (t/c) \cos \Lambda / \beta$$

$$\text{So: } k = 1 + 2 C (t/c) \cos^2 \Lambda / \beta + C^2 \cos^2 \Lambda (t/c)^2 (1 + 5 \cos^2 \Lambda) / 2 \beta^2$$

$$k = 1 + \frac{2 C (t/c) \cos^2 \Lambda}{\sqrt{1 - M_\infty^2 \cos^2 \Lambda}} + \frac{C^2 \cos^2 \Lambda (t/c)^2 (1 + 5 \cos^2 \Lambda)}{2 (1 - M_\infty^2 \cos^2 \Lambda)}$$

The value of k is given in the next figure and compared with other methods and experimental data. A value for C of about 1.1 agrees best with the rather scattered data. When $M \cos \Lambda > 1$, there is not a velocity increase due to t/c and so we take $C=0$.



The fineness ratio of the fuselage affects the fuselage drag by increasing the local velocities and creating a pressure drag. The increase in skin friction due to higher-than-freestream velocities can be estimated by considering the symmetric flow around a body of revolution.

For bodies of revolution, the increase in surface velocity due to thickness is smaller than for 2-D shapes. The maximum velocity can be computed as a function of fineness ratio, assuming a family of fuselage shapes. The actual surface velocity distribution depends strongly on the shape of the body: paraboloids have about half again as much maximum perturbation velocity as ellipsoids, and fuselages with constant cross sections are quite different, but the idea here is to represent the correct trend theoretically, and then obtain empirical constants. The results are shown in the figure below

Form Factor for Bodies

The fineness ratio of the fuselage affects the fuselage drag by increasing the local velocities and creating a pressure drag. The increase in skin friction due to higher-than-freestream velocities can be estimated by considering the symmetric flow around a body of revolution.

For bodies of revolution, the increase in surface velocity due to thickness is smaller than for 2-D shapes.

From potential flow theory, the maximum velocity over an ellipse with thickness ratio t/c is:

$$\Delta u_{\max} / U_0 = t/c.$$

The maximum velocity increase on an ellipsoid of revolution is given by the potential flow solution:

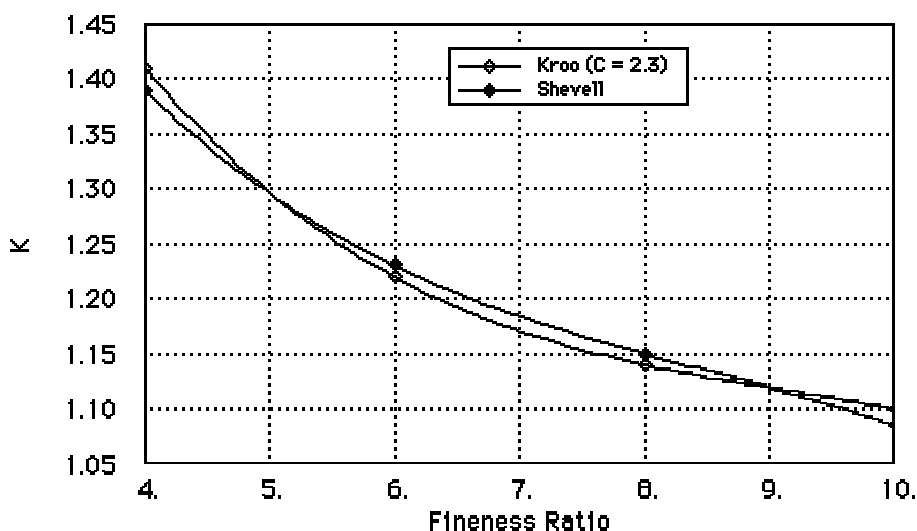
$$\Delta u_{\max} / U_0 = a / (2-a) / (1-M^2)^{0.5}, \text{ where } a = 2(1-M^2) d^2 / D^3 (\tanh^{-1} D - D)$$

and $D = (1 - (1-M^2) d^2)^{0.5}$, and $d = \text{diameter} / \text{length}$.

The actual surface velocity distribution depends strongly on the shape of the body: paraboloids have about half again as much maximum perturbation velocities as ellipsoids, and fuselages with constant cross-sections are quite different, but the idea here is to represent the correct trend theoretically, and then obtain empirical constants. If a sort of average perturbation velocity is represented by $C \Delta u_{\max}$ then the form factor, k , for bodies may be written:

$$k = (1 + C \Delta u_{\max} / U_0)^2.$$

The figure below shows that a factor, $C=2.3$ leads to reasonable agreement with the purely empirical method given by Shevell.



At supersonic speeds, the optimum body shape is closer to a paraboloid, but the velocity distribution is quite different. The maximum velocity no longer occurs at the middle of the body, and the flow is decelerated over more of the area. In fact, based on linear theory, the net form factor is 1.0.

When the body has a non-circular cross-section, the effective diameter may be computed from:

$$D_{\text{effective}} = (4 S / \pi)^{1/2}$$

where S is the maximum cross-sectional area.

Nacelles may also be modeled as bodies of revolution, with an effective fineness ratio given by:

$$\frac{L}{D} = \frac{\text{Nacelle Length} + \text{Inlet Diameter}}{\sqrt{\frac{4}{\pi} \left(A_{\text{max}} - \frac{A_{\text{exit}} + A_{\text{inflow}}}{2} \right)}}$$

Here, A_{exit} = total exit area

A_{inflow} = effective inlet area based on mass flow, approximately = $0.8 A_{\text{inlet}}$

A_{max} = maximum nacelle cross-section area

Typically A_{inlet} is approximately $0.7 A_{\text{max}}$.

Wetted Area Calculations

In order to compute the skin friction drag, it is necessary to multiply this coefficient by the wetted area. For wing-like surfaces, the wetted area is related to the exposed planform area. It is a bit more than twice the exposed area because the arc length over the upper and lower surfaces is a bit longer than the chord:

$$S_{\text{wetted}} \approx 2.0 (1 + 0.2t/c) S_{\text{exposed}}$$

The exposed area is that portion of the wing planform that is exposed to the airflow. It does not include the part of the wing buried in the fuselage, but does include any chord extensions.

For bodies, the wetted area can be computed by adding the contribution of the nose section, constant section, and tapered tail cone. This requires knowledge of the actual fuselage

shape, but for typical transport aircraft, the wetted area of the nose and tail cone may be approximated by:

$$S_{\text{wetted}_{\text{nose}}} = 0.75\pi DL_{\text{nose}} \quad S_{\text{wetted}_{\text{tail}}} = 0.72\pi DL_{\text{tail}}$$

where D is the diameter of the constant section and L is the length of the nose or tail cone. For elliptically-shaped fuselage cross-sections, of width W, and height H, an approximate formula for the perimeter may be used to estimate an effective diameter. One such expression is given below.

$$D_{\text{eff}} = (W/2 + H/2) (64 - 3 R^4) / (64 - 16 R^2)$$

where: $R = (H-W)/(H+W)$

Control surface gap drag

The parasite drag also includes extra drag due to gaps at the control surfaces. This is best estimated based on experimental data. The drag depends on the detailed design of the controls, but for the purposes of this course we take the drag increment to be:

$$f_{\text{gaps}} = .0002 \cos^2 \Lambda S_{\text{affected}}$$

where S_{affected} is the area of the wing, horizontal tail, or vertical tail affected by control surfaces. This is typically about $0.3 S_{\text{wing}}$, $1.0 S_{\text{horiz}}$, and $0.9 S_{\text{vert}}$, but the detailed layout should be used. The correction for sweep is included since the component of the dynamic pressure normal to the gap is the significant term.

Aft-Fuselage Upsweep Drag

The drag due to the upward curvature of the aft fuselage is the sum of a fuselage pressure drag increment due to the upsweep and a drag increment due to a loss of lift. Because of the loss of lift, the airplane must fly at a higher wing lift coefficient in order to maintain the required net airplane C_L . This causes an increase in lift-dependent drag. The total upsweep drag may be written:

$$\Delta C_{D_{\pi\text{upsweep}}} = (\Delta C_{D_{\pi\text{upsweep}}})_{\alpha=\text{const}} + (\Delta C_{L_{\pi\text{upsweep}}})_{\alpha=\text{const}} * (\partial C_D / \partial C_L)$$

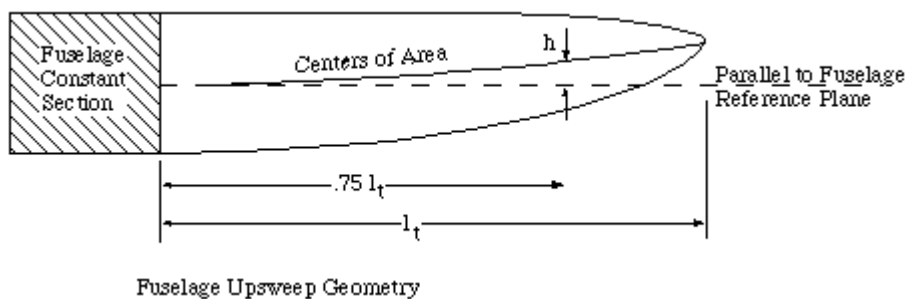
The change in drag with C_L (i.e. dC_D / dC_L) varies with both airplane lift coefficient and Mach number (by virtue of its dependence on the wing compressibility characteristics.) For a first approximation, a single value may be used; 0.04 is typical. The geometric parameter used to correlate upsweep drag with fuselage shape is the vertical displacement of the fuselage centerline in the tail cone above the fuselage reference plane. The vertical position of the center of cross-sectional area is measured, not at the end of the fuselage, but at a point that is located 75% of the total upsweep length. The parameter is thus $(h/l)_{.75}$. This is to minimize the effect of modifications at the very aft end of the fuselage that do not produce much change in the effective upsweep.

The total upsweep drag increment (including each of the two terms discussed previously) increases with the parameter, $(h/l)_{.75 l_t}$, according to the following expression, derived from wind tunnel data:

$$C_{D_{\pi \text{upsweep}}} = 0.075 (h/l)_{.75 l_t}$$

The subscript π denotes the fact that this C_D is nondimensionalized by fuselage maximum cross-sectional area, rather than reference wing area. To obtain the increment in C_D based on wing area, remember to multiply by the ratio of fuselage cross section area to wing area.

Typical values of $C_{D_{\pi \text{upsweep}}}$ are around 0.006. This translates into about 0.0007 based on wing area for a DC-9.



Two points are of interest with regard to aft-fuselage upsweep:

1. Tests of fuselage shapes in the absence of the wing yield results that greatly overestimate the magnitude of the upsweep drag.
2. Wind tunnel test results have indicated that the loss of lift due to upsweep is significantly greater than just the download on the aft fuselage, which suggests that there is a flow change over the wing and forward fuselage due to the aft-fuselage upsweep. Also, the net change in pitching moment due to upsweep is an increased nose-down moment instead of a nose-up moment that might be expected. As a result, the loss in lift does not complement the download on the tail that is required to trim the airplane. In fact, the effect of upsweep is to slightly increase the airplane trim drag.

Nacelle base drag

Among the many items that are included in an explicit manner, one usually estimates the drag increment associated with a small gap between the engine nozzle and the nacelle. Nacelle base drag is a small item, but is representative of the types of drag components that one tries to model in a realistic manner.

Most turbofan engines maintain a gap between the engine nozzle and nacelle of about 1/2 inch. Flow separates and creates a base drag area that may be estimated as the base area (.5 inch times the circumference at the nozzle exit) multiplied by a drag coefficient of about 0.2.

$$\text{So } C_{D_{\text{nacelle_base}}} = 0.5/12 * \pi * D_{\text{exit}} * 0.2 / S_{\text{ref}}$$

with the nozzle exit diameter measured in feet.

Miscellaneous items

In addition to the basic parasite drag of the major components, the drag due to aft-fuselage upsweep, and control surface gaps, there is usually other parasite drag that must be taken into account. This is the drag associated with the air conditioning system, various cooling systems, and the many necessary protuberances that exist on an airplane. The classification of the items to be included in the miscellaneous drag category-and hence to be separately listed-and of the items to be implicitly included in the roughness drag, is somewhat arbitrary. Neither extreme is very attractive. That is, it is impractical to account for every last protuberance on the airplane separately. Yet, on the other hand, some of these items can be significant, so that failure to account for them separately could cause the airplane drag to be underestimated. In the method of this course, such items are included in the miscellaneous drag category. These items include the air conditioning system, flap hinge and track covers, wing fences, and any unique protuberances. Items for which the drag is an implicit part of the 'roughness' markup include cabin leakage, normal antennas, nacelle compartment cooling, canopies, pressure and temperature probes, windshield wipers, and miscellaneous inlets and exhausts.

In accounting for the drag caused by the air conditioning system, only losses associated with the cooling air are to be included. No engine bleed losses are included. However, any thrust recovery resulting from the efficient discharge of cabin air should be included in this evaluation. The parasite drag of any specific protuberance should be calculated by applying the methods discussed previously.

If the design of the airplane has not progressed to the point where a detailed calculation of the drag of the air conditioning system and other items can be made, the drag of these miscellaneous items can be assumed to be about 1.5% of the total airplane parasite drag. This estimate is based on the drag of such items on the DC-8-62, -63, and on the DC-9. The breakdown of the miscellaneous drag for these airplanes is shown in the following table. (Numbers are percent of total airplane parasite drag.)

Item / Airplane	DC-8-62	DC-8-63	DC-9-10	DC-9-20	DC-9-30
Flap Hinge Covers	0.12	0.12	0.69	0.97	0.69
Air Conditioning System (incl. thrust recovery)	0.84	0.82	0.25	0.24	0.24
Vortilon	-	-	0.30	0.29	0.29
Fence and Stall Strip	-	-	0.99	-	-
Miscellaneous	0.25	0.25	-	-	-
Total	1.21%	1.19%	2.23%	1.50%	1.22%

The lift-dependent drag contributions include:

- Vortex Drag
- Lift-Dependent Viscous Drag

Lift-Dependent Drag Items

The total drag coefficient includes the parasite drag and other components:

$$C_D = C_{D_p} + C_{D_{\text{vortex}}} + C_{D_{\text{lift-dependent viscous}}} + C_{D_{\text{compressibility}}}$$

This is sometimes written:

$$C_D = C_{D_p} + C_{D_i} + C_{D_c}$$

The second term, is often called the induced drag, but it includes more than just the inviscid drag associated with induced velocities from the wake. For purposes of this analysis, the "induced" drag is customarily divided into viscous and inviscid parts. The inviscid (vortex) drag includes a zero-lift term due to twist, and lift-dependent parts that depend on the twist and planform. The remaining portion of the "induced" drag, the so-called viscous part, is chiefly due to the increase of skin friction and pressure drag with changes in angle of attack. Such increases come about because of the increased velocities on the upper surface of the wing leading to higher shear stresses and more severe adverse gradients with corresponding increase in pressure drag. As in the case of parasite drag, the "induced" drag also includes several miscellaneous effects not accounted for in a simple theoretical study. Additional empirically-estimated terms arise from fuselage vortex drag, nacelle-pylon interference, changes in trim drag with angle of attack, and a change in drag due to engine power effects (either inlet or exhaust).

Inviscid Part

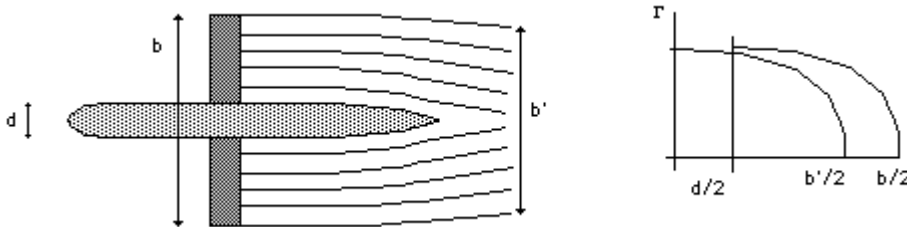
For twisted wings, the inviscid drag may be written:

$$C_{D_{\text{inviscid}}} = C_L^2 / \pi A R u S + a_0 \theta C_L v + (a_0 \theta)^2 w$$

The last term is present at zero-lift and is the zero-lift drag due to twist. The first term is the vortex drag associated with the untwisted wing.

The factor, s , accounts for the added lift-dependent drag caused by the modification of the span loading due to the addition of the fuselage. Its value is presented in the figure below for various ratios of the fuselage width (or diameter) to wing span. The values of this factor are obtained from a solution for the minimum induced drag of a lifting line in combination with a circular fuselage of infinite length and at zero angle of attack.

One may estimate the drag associated with fuselage interference in the following manner:



If the flow were axially symmetric and the fuselage were long, then mass conservation leads to:

$$b'^2 = b^2 - d^2.$$

For minimum drag with fixed lift, the downwash in the far wake should be constant, so the wake vorticity is just like that associated with an elliptical wing with no fuselage of span, b' . The lift on the wing-fuselage system is computable from the far-field vorticity, so the span efficiency is:

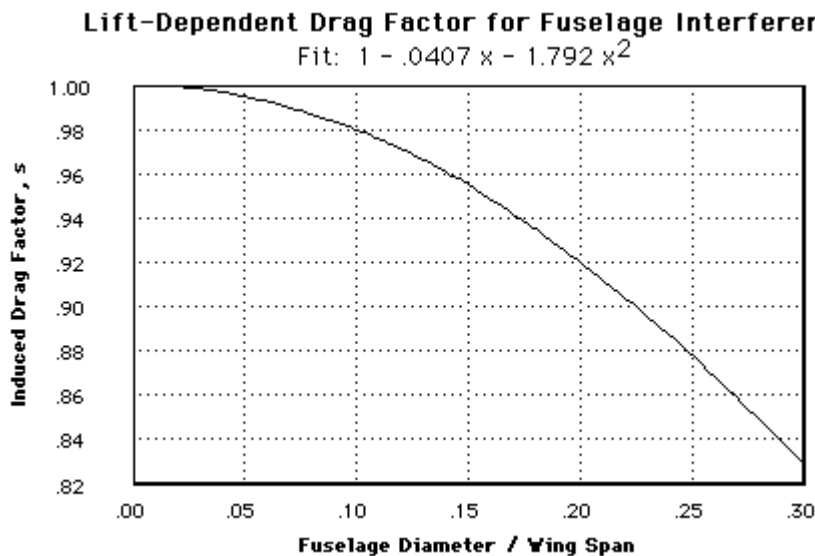
$$e = 1 - d^2 / b^2.$$

In practice, one does not achieve this much lift on the fuselage. Assuming a long circular fuselage and computing the lift based on images, the resulting induced drag increment is about twice the simple theoretical value, so:

$$s = 1 - 2 d^2 / b^2.$$

Although the analysis was made only for a mid-wing location, the results are used in this method for all wing locations. These results are probably slightly conservative for application to low-wing designs. However, the use of these results for wing installations with large root incidence angles does not fully predict the detrimental effect of the fuselage on the wing span-load distribution. It has been shown that with large wing

incidences there is a much greater deficiency in the lift "carry-over" on the fuselage. The value of 's' is usually between .965 and .985. For initial studies assuming a value of .975 will lead to no more than a 1% error in lift dependent drag, but if the chart below is available, use that.



Apart from this factor, the expression for inviscid drag of the wing alone shows how planform and twist affect the drag. Simple finite wing theory shows that if the distribution of lift over the wing is elliptical, the inviscid drag is minimized with a given span, lift, and flight condition. We can make the span loading nearly elliptical with suitable choices of wing planform and twist and so should be able to approach the ideal minimum value quite closely. We can use the expression above, in fact, to solve for the twist angle that produces the minimum C_{Di} for a given planform. Generally, twists that are somewhat greater than that required for minimum induced drag are used. This is often done to improve handling or reduce induced drag at low speeds. Thus, the total inviscid drag is somewhat greater than the ideal minimum: $C_L^2 / \pi AR$.

For most transport-like configurations taper ratios are chosen in the 0.20 to 0.35 region where the value of u is close to 0.99. (The values of u, v, and w depend only on the planform.) The lift-dependent twist term can actually contribute a negative drag increment. If the taper and sweep are higher than ideal, for example, the wing can be "washed-out" (negative twist) to bring the loading closer to elliptical.

Rather than evaluate the u, v, and w terms in the expression above, designers generally now rely on computations of a specific wing planform and twist distribution to estimate the vortex drag. If a wing-body analysis code is available, the lift carry-over can be estimated well and there is no need for the fuselage s-term either. In many cases, though, initial wing design studies will be performed without the fuselage and the fuselage correction factor, s, applied to these results.

Trim Drag

When the tail of an airplane carries some load, several drag components are increased: the tail itself has vortex drag and lift-dependent viscous drag, but the lift of the wing must be changed to obtain a specified airplane C_L :

$$C_{L_{\text{Airplane}}} = C_{L_{\text{Airplane}}} + C_{L_{\text{tail}}} (S_{\text{tail}} / S_{\text{wing}})$$

The increase in wing C_L means that the wing vortex and lift-dependent viscous drag increases. In addition, wing compressibility drag is affected.

To compute this, we first must calculate the lift carried by the tail. For most transport aircraft without active controls this is about 5% of the airplane lift, but in the wrong (downward) direction. We could then compute the vortex drag of the combined wing/tail system and then add in viscous and compressibility increments. The difficulty with this is that unless we know the airplane center of gravity (CG) location, we cannot compute the tail load and in the early stages of the analysis, we do not know the airplane CG location. Sometimes we make rough estimates of the CG. When this is not possible, we can rely on more detailed computations done on other aircraft which show trim drag of about 1% to 2% of airplane drag. Airplane designs can easily be created with very high trim drag values, though. We will discuss this in connection with tail design in subsequent chapters.

Viscous Part

Over most of the flight regime of interest, the viscous part of the "induced" drag may be approximated by a parabolic variation with C_L . Thus we write:

$$C_{D_{i_viscous}} = K C_{D_p} C_L^2$$

Ideally, this drag contribution should be estimated for the individual airplane components, with factors such as the influence of wing leading edge geometry, wing camber, wing thickness ratio, wing sweep, pylon interference, fuselage upsweep, tail induced drag, power effects, etc. taken into account. Since the information required to do this usually does not exist in preliminary design, it is assumed that a new airplane will be similar enough to previous airplanes that the viscous part of the lift-dependent drag can be represented by the equation above, with the K factor determined from previous flight test data. The wing contribution, including the effect of sweep, is included separately from the contributions of the other components. The form of the expression for lift-dependent viscous drag may be derived by combining simple sweep theory with the equation for airfoil superelevations due to circulation.

The value of the factor K has been determined from flight test data for the DC-8-62 and 63

and for the DC-9-10, -20, and -30 airplanes to be approximately 0.38.

When each of these effects is added together, the total drag is seen to vary quadratically with C_L . In fact, apart from the lift dependent twist term, the drag polar is a parabola and would form a straight line when plotted vs. C_L^2 . Since the lift-dependent twist term is usually very small, we expect that the C_D vs. C_L^2 will be nearly straight. This is often the case. The drag polar can thus be approximated, over most of the range of interest by the two-parameter expression:

$$C_D = C_{D_p} + C_L^2 / \pi A R e$$

'e' is a parameter which expresses the total variation of drag with lift. It is sometimes called the span efficiency factor or Oswald efficiency factor after Dr. W.B. Oswald who first used it. It would be 1.0 for an elliptically-loaded wing with no lift-dependent viscous drag, but for practical aircraft 'e' varies from about 0.75 to 0.90.

We can predict the value of 'e' by computing the inviscid drag from a lifting surface method and adding the lift-dependent viscous drag:

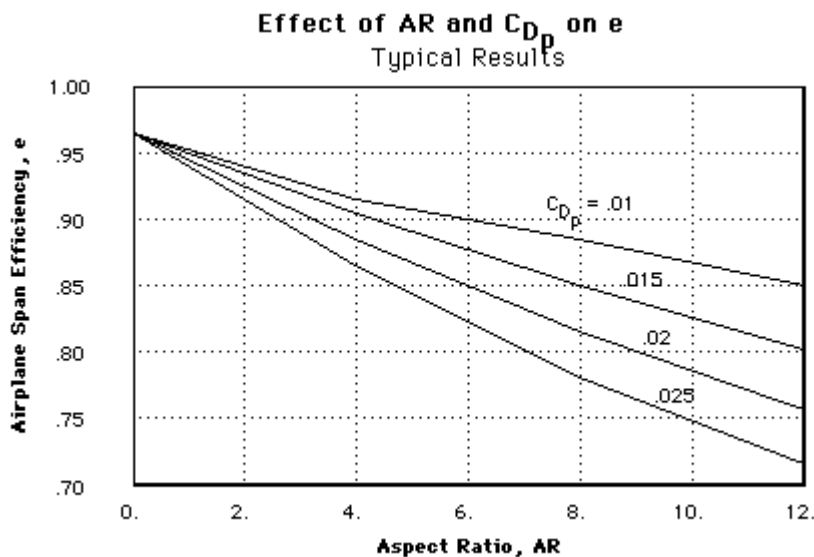
$$C_D = C_{D_p} + C_{D_{i_inviscid}} + K C_{D_p} C_L^2 = C_{D_p} + C_L^2 / (\pi A R e_{inviscid}) + K C_{D_p} C_L^2$$

$$\text{So if } C_D = C_{D_p} + C_L^2 / (\pi A R e)$$

then:

$$e = \frac{1}{\pi A R \left(\frac{1}{\pi A R e_{inviscid}} + K C_{D_p} \right)} = \frac{1}{\frac{1}{e_{inviscid}} + \pi A R K C_{D_p}}$$

The figure below shows a typical variation in e with aspect ratio, sweep, and C_{D_p} . The chart was constructed by assuming $u = 0.99$ and $s = 0.975$, and it works quite well, although the calculation should be done in detail for a specific airplane. C_{D_p} for jet transports typically varies from about .0140 for aircraft with small ratios of body wetted area to wing wetted area (707 or DC-8) to .0210 for short range aircraft with a relatively large fuselage. The wide-body tri-jets lie in the middle of this range. Note that this plot shows typical values, the actual value of 'e' for a particular airplane should be computed as described above.



Aircraft with wing-mounted propellers have a further reduction in ' e ' due to the downwash behind inclined propellers. The exact effect is difficult to calculate but a reduction of about 4% is reasonable.

The wave drag contributions may include:

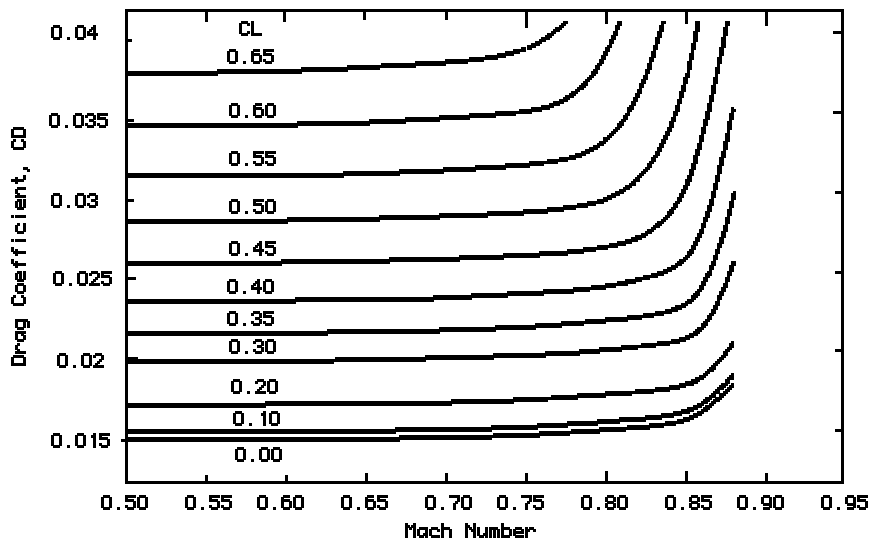
- Transonic compressibility drag
- Supersonic volume wave drag
- Supersonic lift-dependent wave drag

Transonic Compressibility Drag

This section deals with the effect of Mach number on drag from subsonic speeds through transonic speeds. We concentrate on some of the basic physics of compressible flow in order to estimate the incremental drag associated with Mach number.

The chapter is divided into the following sections:

Compressibility Drag: Introduction



The low speed drag level is often defined at a Mach number of 0.5, below which the airplane drag coefficient at a given lift coefficient is generally invariant with Mach number. The increase in the airplane drag coefficient at higher Mach numbers is called compressibility drag. The compressibility drag includes any variation of the viscous and vortex drag with Mach number, shock-wave drag, and any drag due to shock-induced separations. The incremental drag coefficient due to compressibility is designated C_{D_c} .

In exploring compressibility drag, we will first limit the discussion to unswept wings. The effect of sweepback will then be introduced. For aspect ratios above 3.5 to 4.0, the flow over much of the wing span can be considered to be similar to two-dimensional flow. Therefore, we will be thinking at first in terms of flow over two-dimensional airfoils.

When a wing is generating lift, velocities on the upper surface of the wing are higher than the freestream velocity. As the flight speed of an airplane approaches the speed of sound, i.e., $M > 0.65$, the higher local velocities on the upper surface of the wing may reach and even substantially exceed $M = 1.0$. The existence of supersonic local velocities on the wing is associated with an increase of drag due to a reduction in total pressure through shockwaves and due to thickening and even separation of the boundary layer due to the local but severe adverse pressure gradients caused by the shock waves. The drag increase is generally not large, however, until the local speed of sound occurs at or behind the 'crest' of the airfoil, or the 'crestline' which is the locus of airfoil crests along the wing span. The crest is the point on the airfoil upper surface to which the freestream is tangent, Figure 1. The occurrence of substantial supersonic local velocities well ahead of the crest does not lead to significant drag increase provided that the velocities decrease below sonic forward of the crest.

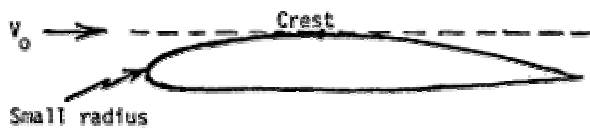


Fig. 1 Definition of the Airfoil Crest

A shock wave is a thin sheet of fluid across which abrupt changes occur in p , ρ , V and M . In general, air flowing through a shock wave experiences a jump toward higher density, higher pressure and lower Mach number. The effective Mach number approaching the shock wave is the Mach number of the component of velocity normal to the shock wave. This component Mach number must be greater than 1.0 for a shock to exist. On the downstream side, this normal component must be less than 1.0. In a two-dimensional flow, a shock is usually required to bring a flow with $M > 1.0$ to $M < 1.0$. Remember that the velocity of a supersonic flow can be decreased by reducing the area of the channel or streamtube through which it flows, When the velocity is decreased to $M = 1.0$ at a minimum section and the channel then expands, the flow will generally accelerate and become supersonic again. A shock just beyond the minimum section will reduce the Mach number to less than 1.0 and the flow will be subsonic from that point onward.

Whenever the local Mach number becomes greater than 1.0 on the surface of a wing or body in a subsonic freestream, the flow must be decelerated to a subsonic speed before reaching the trailing edge. If the surface could be shaped so that the surface Mach number is reduced to 1.0 and then decelerated subsonically to reach the trailing edge at the surrounding freestream pressure, there would be no shock wave and no shock drag. This ideal is theoretically attainable only at one unique Mach number and angle of attack. In general, a shock wave is always required to bring supersonic flow back to $M < 1.0$. A major goal of transonic airfoil design is to reduce the local supersonic Mach number to as close to $M = 1.0$ as possible before the shock wave. Then the fluid property changes through the shock will be small and the effects of the shock may be negligible. When the Mach number just ahead of the shock becomes increasingly larger than 1.0, the total pressure losses across the shock become greater, the adverse pressure change through the shock becomes larger, and the thickening of the boundary layer increases.

Near the nose of a lifting airfoil, the streamtubes close to the surface are sharply contracted signifying high velocities. This is a region of small radius of curvature of the surface, Figure 1, and the flow, to be in equilibrium, responds like a vortex flow, i.e. the velocity drops off rapidly as the distance from the center of curvature is increased. Thus the depth, measured perpendicular to the airfoil surface, of the flow with $M > 1.0$ is small. Only a small amount of fluid is affected by a shock wave in this region and the effects of the total pressure losses caused by the shock are, therefore, small. Farther back on the airfoil, the curvature is much less, the radius is larger and a high Mach number at the surface persists much further out in the stream. Thus, a shock affects much more fluid. Furthermore, near

the leading edge the boundary layer is thin and has a full, healthy, velocity profile. Toward the rear of the wing, the boundary layer is thicker, its lower layers have a lower velocity and it is less able to keep going against the adverse pressure jump of a shock. Therefore, it is more likely to separate.

For the above reasons supersonic regions can be carried on the forward part of an airfoil almost without drag. Letting higher supersonic velocities create lift forward allows the airfoil designer to reduce the velocity at and behind the crest for any required total lift and this is the crucial factor in avoiding compressibility drag on the wing.

The unique significance of the crest in determining compressibility drag is largely an empirical matter although many explanations have been advanced. One is that the crest divides the forward facing portion of the airfoil from the aft facing portion. Supersonic flow, and the resulting low pressures (suction) on the aft facing surface would contribute strongly to drag. Another explanation is that the crest represents a minimum section when the flow between the airfoil upper surface and the undisturbed streamlines some distance away is considered, figure 2. Thus, if $M \geq 1.0$ at crest, the flow will accelerate in the diverging channel behind the crest, this leads to a high supersonic velocity, a strong suction and a strong shock.

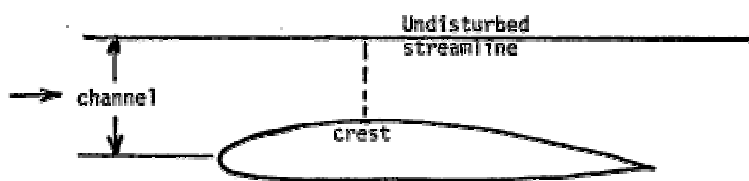


Fig. 2 One View of the Airfoil Crest

The freestream Mach number at which the local Mach number on the airfoil first reaches 1.0 is known as the critical Mach number. The freestream Mach number at which $M = 1.0$ at the airfoil crest is called the crest critical Mach number, M_{cc} . The locus of the airfoil crests from the root to the tip of the wing is known as the crestline.

Empirically it is found that the drag of conventional airfoils rises abruptly at 2 to 4% higher Mach number than that at which $M = 1.0$ at the crest (supercritical airfoils are a bit different as discussed briefly later). The Mach number at which this abrupt drag rise starts is called the drag divergence Mach number, M_{Div} . This is a major design parameter for all high speed aircraft. The lowest cost cruising speed is either at or slightly below M_{Div} depending upon the cost of fuel.

Since C_p at the crest increases with C_L , M_{Div} generally decreases at higher C_L . At very low C_L , the lower surface becomes critical and M_{Div} decreases, as shown in Figure 3.

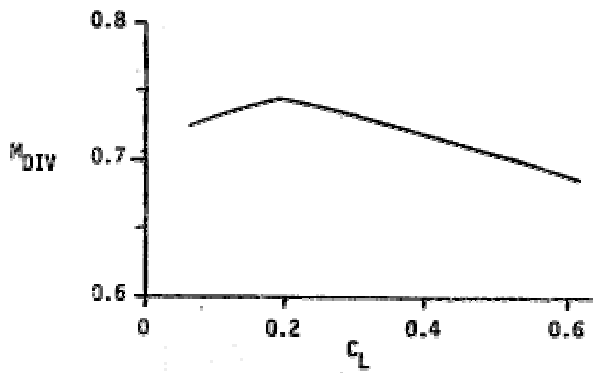


Fig. 3 Typical Variation of Airfoil M_{Div} with C_L

The drag usually rises slowly somewhat below M_{Div} due to the increasing strength of the forward, relatively benign shocks and to the gradual thickening of the boundary layer. The latter is due to the shocks and the higher adverse pressure gradients resulting from the increase in airfoil pressures because C_p at each point rises with $(1-M_0^2)^{-1/2}$. The nature of the early drag rise is shown in Figure 4.

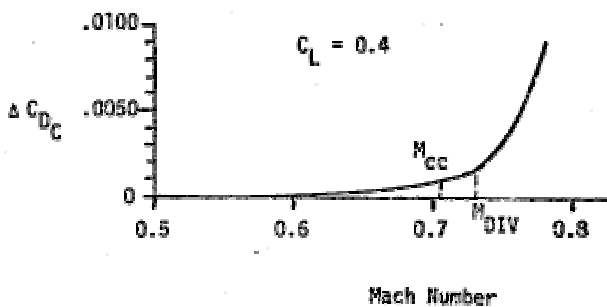


Figure 4. Typical Variation Of C_{Dc} with Mach Number

There is also one favorable drag factor to be considered as Mach number is increased. The skin friction coefficient decreases with increasing Mach number as shown in figure 5. Below Mach numbers at which waves first appear and above about $M=0.5$, this reduction just about increased drag from the higher adverse pressure gradient due to Mach. Therefore, the net effect on drag coefficient due to increasing Mach $M=0.5$ is usually negligible until some shocks occur on the wing or favorable effect of Mach number on skin friction is very significant sonic Mach number, however.

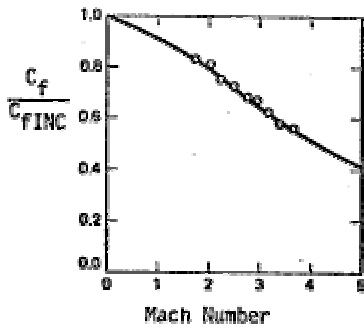


Figure 5. The Ratio of the Skin Friction Coefficient in Compressible Turbulent Flow to the Incompressible Value at the Same Reynolds Number

Predicting M_{div} and M_{cc}

Compressibility Drag: M_{Div}

Since M_{Div} is 2 to 4% above M_{cc} (we shall see that the '2 to 4%' is dependent on wing sweepback angle), we can predict the drag rise Mach number, M_{Div} if we can predict M_{cc} . If we can identify the pressure drop or more conveniently the local pressure coefficient, C_p , required on an airfoil to accelerate the flow locally to exactly the speed of sound, measured or calculated crest pressures can be used to determine the freestream Mach numbers at which $M = 1.0$ at the crest. If p is the pressure at a point on an airfoil of an unswept wing, the pressure coefficient is

$$C_p = (p - p_\infty) / q_\infty$$

The C_p may be expressed in terms of the local and freestream Mach numbers. Under the assumption of adiabatic flow:

$$C_p = \frac{1}{0.7 M_\infty^2} \left[\left(\frac{1 + 0.2 M_\infty^2}{1 + 0.2 M^2} \right)^{3.5} - 1 \right]$$

By definition, when local Mach number $M = 1.0$, $C_p = C_p^*$, the critical pressure coefficient. Thus,

$$C_p^* = \frac{1}{0.7 M_\infty^2} \left[\left(\frac{1}{1.2} + \frac{M_\infty^2}{6.0} \right)^{3.5} - 1 \right]$$

Compressibility Drag: 3D Effects and Sweep

The previously described method applies to two-dimensional airfoils, but can be used effectively in estimating the drag rise Mach number of wings when the effects of sweep and other 3-D effects are considered.

Average t/c

In Figure 7 the mean thickness ratio t/c is the average t/c of the exposed wing weighted for wing area affected just as the mean aerodynamic chord, MAC, is the average chord of the wing weighted for wing area affected. The mean thickness ratio of a trapezoidal wing with a linear thickness distribution is given by:

$$t/c_{avg} = (t_{root} + t_{tip}) / (C_{root} + C_{tip})$$

This equation for t/c_{avg} is based on a linear thickness (not linear t/c) distribution. This results from straight line fairing on constant % chord lines between airfoils defined at root and tip. The same equation is valid on a portion of wing correspondingly defined when the wing has more than two defining airfoils. The entire wing t/c_{avg} can then be determined by averaging the t/c_{avg} of these portions, weighting each t/c_{avg} by the area affected. Note that C_{root} and C_{tip} are the root and tip chords while t_{root} and t_{tip} are the root and tip thicknesses. b is the wing span and y is the distance from the centerline along the span.

Sweptback Wings

Almost all high speed subsonic and supersonic aircraft have sweptback wings. The amount of sweep is measured by the angle between a lateral axis perpendicular to the airplane centerline and a constant percentage chord line along the semi-span of the wing. The latter is usually taken as the quarter chord line both because subsonic lift due to angle of attack acts at the quarter chord and because the crest is usually close to the quarter chord.

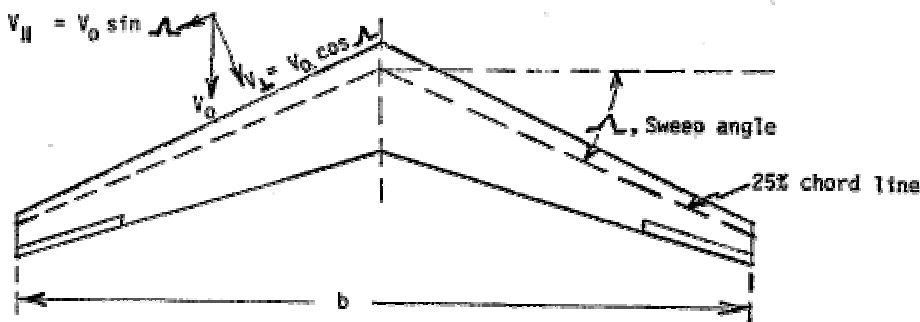


Figure 8. Velocity Components Affecting a Sweptback Wing

Sweep increases M_{cc} and M_{Div} . The component of the freestream velocity parallel to the wing, $V_{||}$, as shown in figure 8 does not encounter the airfoil curvatures that produce increased local velocities, reduced pressures, and therefore lift. Only the component

perpendicular to the swept span, V_n , is effective. Thus on a wing with sweep angle, Λ :

$$V_{0\text{eff}} = V_0 \cos \Lambda$$

$$M_{0\text{eff}} = M_0 \cos \Lambda$$

$$q_{0\text{eff}} = q_0 \cos^2 \Lambda$$

The meaningful crest critical Mach number, M_{cc} , is the freestream Mach number at which the component of the local Mach number at the crest, perpendicular to the isobars, first reaches 1.0. These isobars or lines of constant pressure coincide closely with constant percent chord lines on a well-designed wing.

Since $q_{0\text{effective}}$ is reduced, the C_L based on this q and the C_p at the crest, also based on $q_{0\text{effective}}$ will increase, and M_{cc} and M_{Div} will be reduced. Furthermore, the sweep effect discussion so far has assumed that the thickness ratio is defined perpendicular to the quarter chord line. Usual industry practice is to define thickness ratio parallel to the freestream. This corresponds to sweeping the wing by shearing in planes parallel to the freestream rather than by rotating the wing about a pivot on the wing centerline. When the wing is swept with constant freestream thickness ratio, the thickness ratio perpendicular to the quarter chord line increases. The physical thickness is constant but the chord decreases. The result is a further decrease in sweep effectiveness below the pure cosine variation. Thus, there are several opposing effects, but the favorable one is dominant.

In addition to increasing M_{cc} , sweepback slightly increases the speed increment between the occurrence of Mach 1.0 flow at the crest and the start of the abrupt increase in drag at M_{Div} . Using a definition for M_{Div} as the Mach number at which the slope of the C_D vs. M_0 curve is 0.05 (i.e. $dC_D/dM = 0.05$), the following empirical expression closely approximates M_{Div} :

$$M_{Div} = M_{cc} [1.02 + .08 (1 - \cos \Lambda)]$$

Other 3-D Effects

The above analysis is based on two-dimensional sweep theory and applies exactly only to a wing of infinite span. It also applies well to most wings of aspect ratio greater than four except near the root and tip of the wing where significant interference effects occur.

The effect of the swept wing is to curve the streamline flow over the wing as shown in Figure 9. The curvature is due to the deceleration and acceleration of the flow in the plane perpendicular to the quarter chord line.

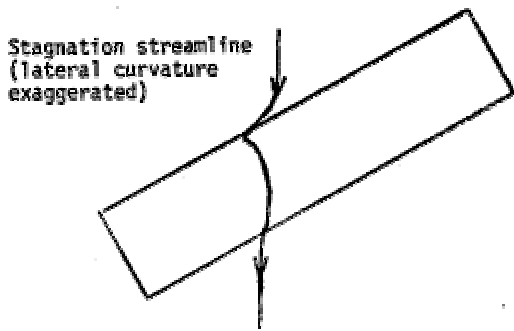


Figure 9. Stagnation Streamline with Sweep

Near the wing tip the flow around the tip from the lower to upper surface obviously alters the effect of sweep. The effect is to unsweep the spanwise constant pressure lines known as isobars. To compensate, the wing tip may be given additional structural sweep, Figure 10.

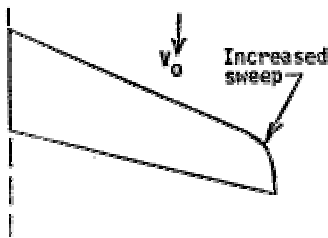


Figure 10. Highly Swept Wing Tip

It is at the wing root that the straight fuselage sides more seriously degrade the sweep effect by interfering with curved flow of figure 9. Airfoils are often modified near the root to change the basic pressure distribution to compensate for the distortions to the swept wing flow. Since the fuselage effect is to increase the effective airfoil camber, the modification is to reduce the root airfoil camber and in some cases to use negative camber. The influence of the fuselage then changes the altered root airfoil pressures back to the desired positive camber pressure distribution existing farther out along the wing span.

This same swept wing root compensation can be achieved by adjusting the fuselage shape to match the natural swept wing streamlines. This introduces serious manufacturing and passenger cabin arrangement problems so that the airfoil approach is used for transports. Use of large fillets or even fuselage shape variations is appropriate for fighters. The designing of a fuselage with variable diameter for transonic drag reasons is sometimes called 'coke-bottling'. At $M = 1.0$ and above, there is a definite procedure for this minimization of shock wave drag. It is called the "area rule" and aims at arranging the airplane components and the fuselage cross-sectional variation so that the total aircraft cross-sectional area, in a plane perpendicular to the line of flight, has a smooth and prescribed variation in the longitudinal (flight) direction. This is discussed further in the section on supersonic drag.

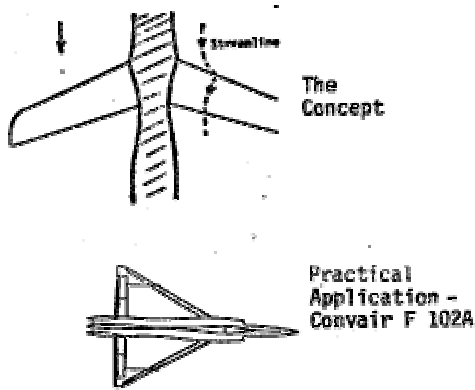


Figure 11. 'Coke-Bottled' Fuselage

The estimates provided by Figure 7 and the equation for M_{Div} assume that the wing root intersection has been designed to compensate for the 'unsweeping' effect of the fuselage either with airfoil or fuselage fairing treatment. If this is not done, M_{Div} will be reduced or there will be a substantial drag rise at Mach numbers lower than M_{Div} . For all aircraft there is some small increase in drag coefficient due to compressibility at Mach numbers below M_{Div} as illustrated in Figure 4.

Compressibility Drag: Computing C_{D_c}

The increment in drag coefficient due to compressibility, C_{D_c} , from its first appearance to well beyond M_{Div} can be estimated from Figure 12 where C_{D_c} is normalized by dividing by $\cos^3 L$ and plotted against the ratio of freestream Mach number, M_0 to M_{cc} . Actual aircraft may have slightly less drag rise than indicated by this method if very well designed. A poor design could easily have higher drag rise. The differences arise from early shocks on some portion of the wing or other parts of the airplane. Figure 12 is an empirical average of existing transport aircraft data.

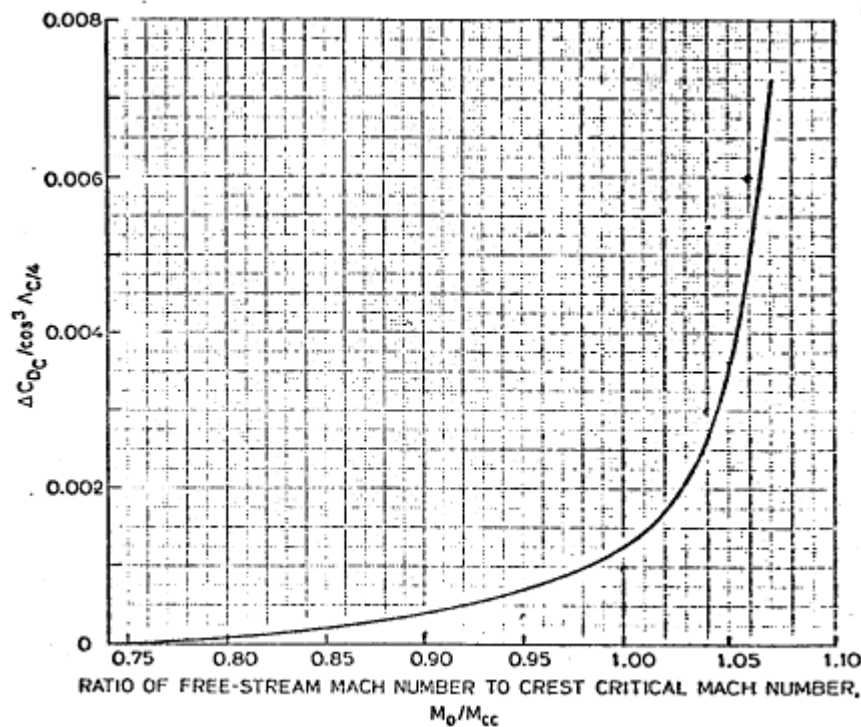


Figure 12 Incremental Drag Coefficient Due To Compressibility

In summary, the method for estimating compressibility drag is as follows:

1. Determine the crest critical Mach number for the values of lift coefficient being studied from figure 7 for the appropriate values of the wing quarter chord sweep angle and the average thickness ratio for the exposed part of the wing.
2. Determine the incremental drag coefficient due to compressibility from figure 12 for the crest-critical Mach numbers from step 1.

When this method is used, the following limitations should be kept in mind:

1. The method assumes that the dominant factor in the airplane compressibility drag characteristics at cruising conditions is the wing. This means that the other components must have drag-divergence Mach numbers higher than that of the wing and that interference must be kept to a minimum in order for this method to be applicable.
2. The estimates for the crest critical Mach number in terms of the wing sweep angle, thickness ratio measured in the freestream direction, and lift coefficient are based on peaky airfoil sections. This method would not be reliable for significantly different types of airfoil sections.

One further note is in order. The expression "drag divergence Mach number" or M_{Div} is the Mach number at which the drag begins to rise abruptly. It is usually desirable to cruise close to M_{Div} .

Numerous definitions of 'rise abruptly' have been used including:

- a. $M_{Div} = M$ for $C_{Dc} = .0014$, or some other value varying from .0010 to .0025
- b. $M_{Div} = M$ for $dC_D/dM = .03$ or .05 or 0.10
- c. $M_{Div} = M$ at constant lift coefficient for $M C_L/C_D$, a term in the range expression, equals 99% of the maximum $M C_L/C_D$

Method (c) is most meaningful and corresponds approximately to $(dC_D/dM) = .03$ and usually to $C_{Dc} = .0012$ to .0016.

The M_{Div} for bodies can be related to the occurrence of critical Mach number, or sonic velocity, at or behind the longitudinal station of maximum cross-sectional area. This is analogous to the crest theory of M for airfoils. Another factor is present on bodies, however, namely that the expanding forward portion of the body tends to thin the boundary layer and make it less likely to separate. Generally the M_{Div} of bodies can be assumed to be about 3% above the Mach number at which sonic velocity occurs at the maximum cross-sectional area.

Notation for this chapter:

C_L Airplane lift coefficient

C_{Dc} Incremental drag coefficient due to compressibility

M_{cc} Crest critical Mach number, the flight Mach number at which the velocities at the crest of the wing in a direction normal to the isobars becomes sonic

M_0 The flight Mach number

β Prandtl-Glauert Factor $(1-M_0)^{1/2}$

t/c Average thickness to chord ratio, in the freestream direction, for the exposed part of the wing

V_0 The flight speed

V Surface perturbation velocity

$c/4$ Wing quarter-chord sweepback angle, degrees

c Sweepback angle of isobars at wing crest, degrees

γ Ratio of specific heats, 1.40 for air.

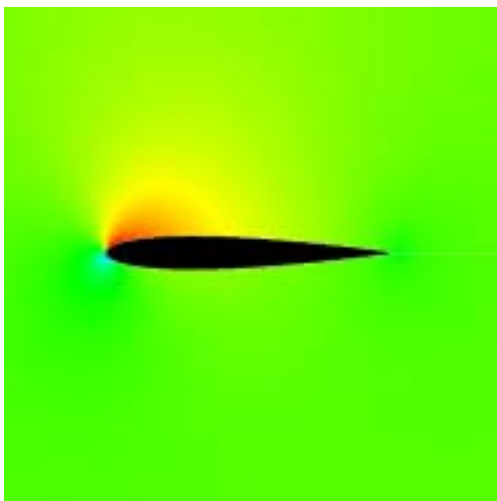
Compressibility Drag Example

NACA 0012 Airfoil, $C_L = 0.5$

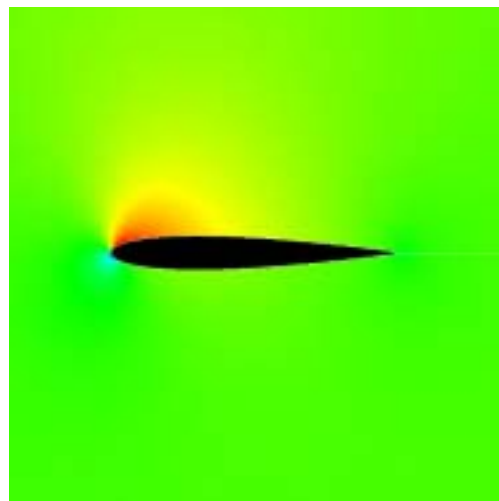
The following figures show the development of the flow field around a two-dimensional NACA 0012 airfoil section in the Mach number range 0.50 - 0.90. The data was obtained with a two-dimensional Euler flow solver. Since the program solves the Euler equations, only the compressibility drag due to the presence of shock waves is accounted for. Other effects such as shock-induced separation cannot be predicted with this model.

The different shades of color represent the changing values of Mach number in the flow domain. Red represents regions of *high* Mach number (mostly on the upper surface where the flow is being accelerated) and blue represents regions of *low* Mach number (mostly at the stagnation point regions in the leading and trailing edge areas).

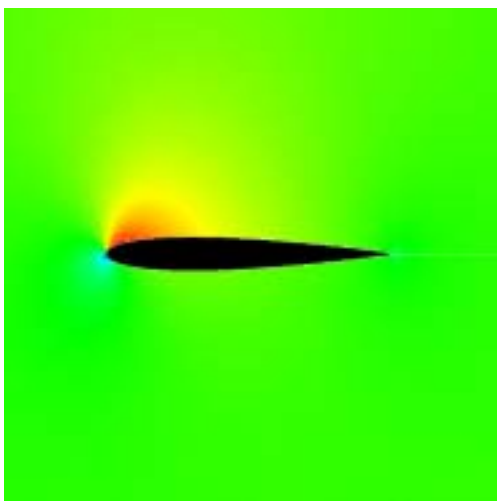
The sonic line (contour line where the Mach number is exactly 1.0) is shown as a faint white line when sonic flow exists. The flow is presented for the following Mach numbers:



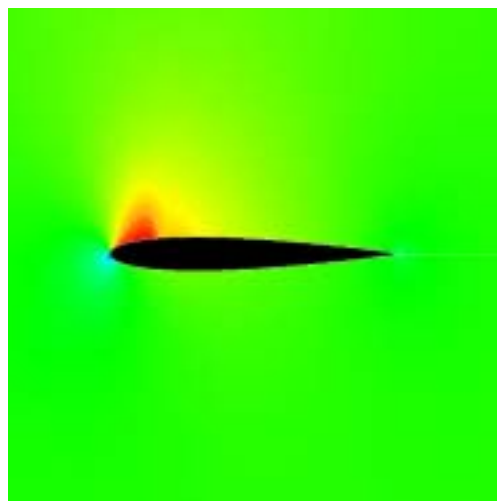
M = 0.50



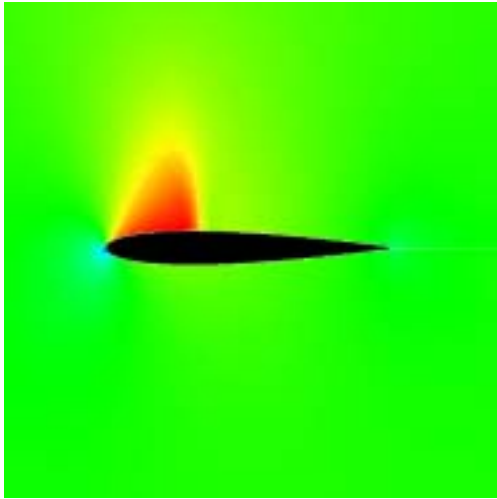
M = .55



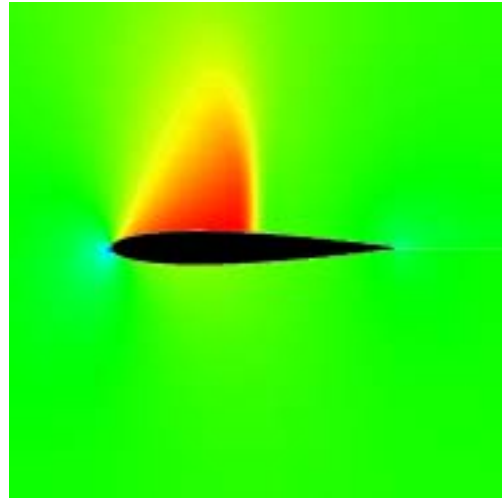
M = 0.60



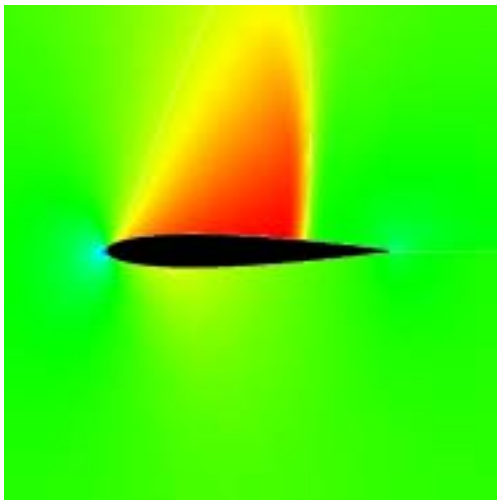
M = .65



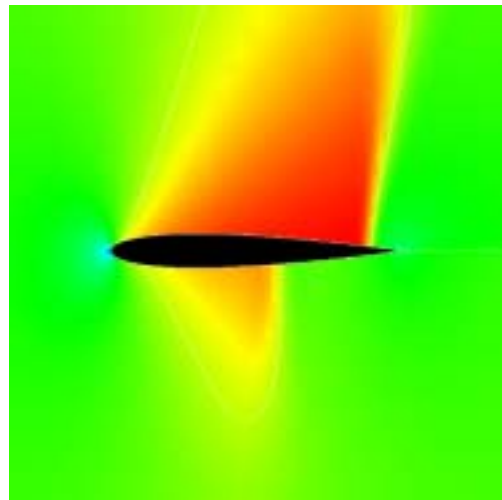
M=0.70



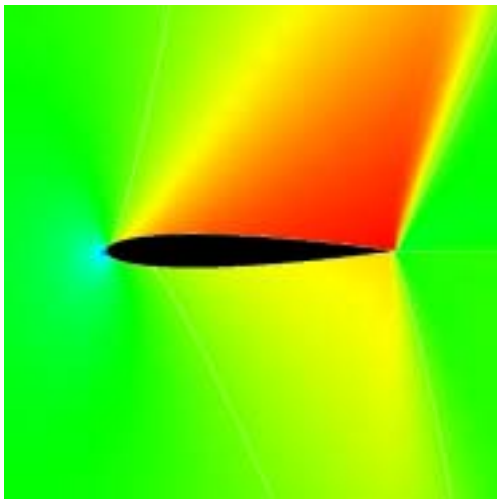
M=.75



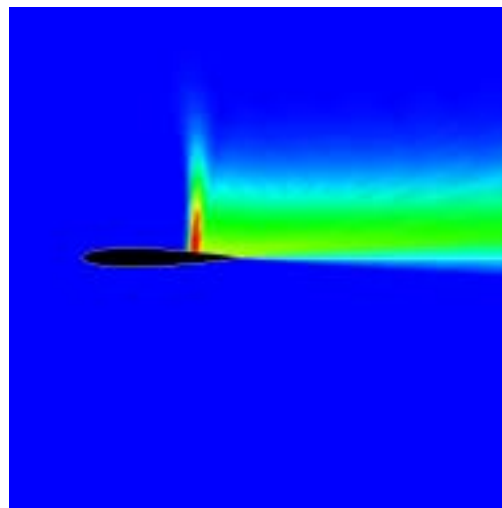
M=0.80



M=.85



M=0.90

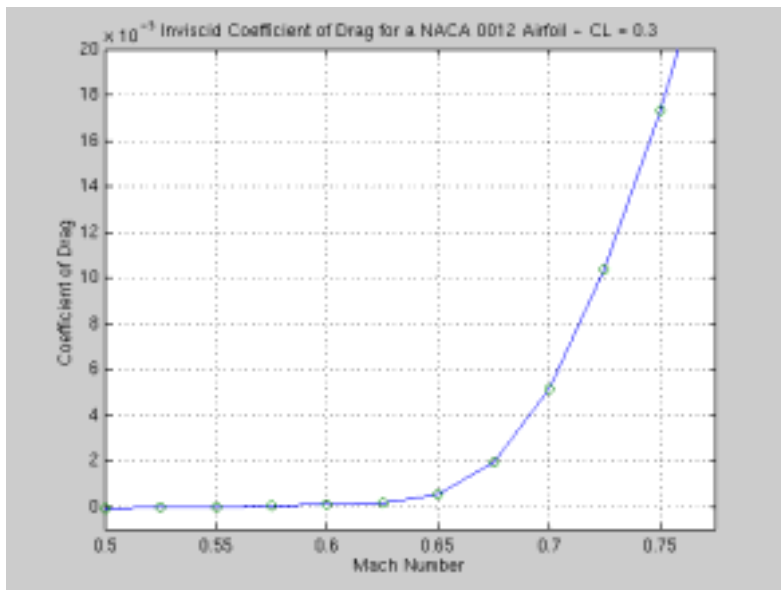


entropy

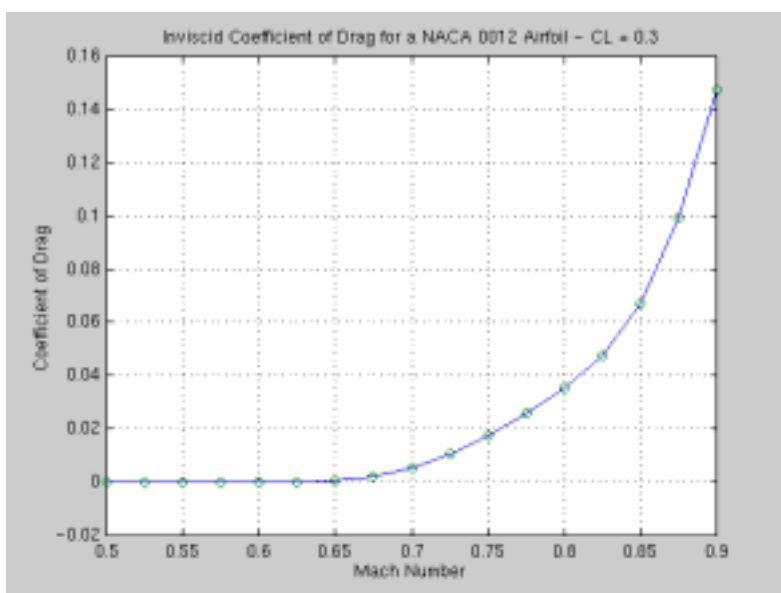
The appearance of drag in the compressible regime is directly related to the existence of shock waves and the consequent total pressure losses and entropy creation. This image shows the entropy field for the Mach 0.80 condition. As you can see, in an inviscid calculation, entropy is created at the shock and is convected downstream with the flow. Ahead of the shock the dark blue color indicates that no entropy has been generated and

that the level of entropy there is that of the free stream. In a viscous calculation, additional entropy would be generated in the boundary layer.

With an average angle of attack of 3.966 degrees for these flow solutions, you can get an idea of the location of the crest for this airfoil. The following two figures are plots of the coefficient of drag of the airfoil vs. Mach number at two different scales. From these plots and the images of the flow field, you should be able to get an idea of the relationships between *critical Mach number*, M_c , *crest critical Mach number*, M_{cc} , and *divergence Mach number*, M_{div} .



Notice that the scale in the following plot is quite large. Drag divergence occurs somewhere between Mach 0.65 and 0.70 for this airfoil. For carefully designed supercritical airfoils M_{div} achieves a higher value (around 0.80 - 0.85).



Supersonic Drag

As the Mach number increases further, the drag associated with compressibility continues to increase. For most commercial aircraft this limits the economically feasible speed. If one is willing to pay the price for the drag associated with shock waves, one can increase the flight speed to Mach numbers for which the above analysis is not appropriate.

In supersonic flow an aircraft has lift and volume-dependent wave drag in addition to the viscous friction and vortex drag terms:

$$\text{Drag} = \underbrace{q K S}_{\text{friction}} + \underbrace{\frac{\text{Lift}^2}{q \pi b^2}}_{\text{vortex}} + \underbrace{\frac{M^2 - 1}{2} \frac{\text{Lift}^2}{q \pi l^2}}_{\text{lift-dependent wave}} + \underbrace{q \frac{128}{\pi} \frac{\text{Volume}^2}{l^4}}_{\text{volume wave}}$$

This approximate expression was derived by R.T. Jones, Sears, and Haack for the minimum drag of a supersonic body with fixed lift, span, length, and volume.

The expression holds for low aspect ratio surfaces. Notice that unlike the subsonic case, the supersonic drag depends strongly on the airplane length, l . This section describes some of the approaches to computing supersonic wave drag components including Volume Wave Drag and Wave Drag Due to Lift:

Volume Wave Drag

One can compute the wave drag on a body of revolution relatively easily. For a paraboloid of revolution the drag coefficient based on frontal area is:

$$C_{D\pi} = \frac{10.67}{(L/D)^2}$$

For a body with minimum drag with a fixed length and maximum diameter, the result is:

$$C_{D\pi} = \frac{9.87}{(L/D)^2}$$

Note that even with a fineness ratio ($L/D = \text{length} / \text{diameter}$) of 10, the drag coefficient is about 0.1 -- a large number considering that typical total fuselage drag coefficients based on frontal area are around 0.2.

Minimum Drag Bodies

In the 1950's Sears and Haack solved for the shape of a body of revolution with minimum wave drag. These results provide guidance for initial estimates of volume wave drag, even before the detailed geometry is known. Two solutions are shown below.

- | | |
|---------------------------------------|-----------------------------|
| 1. Given maximum diameter and length: | 2. Given volume and length: |
|---------------------------------------|-----------------------------|

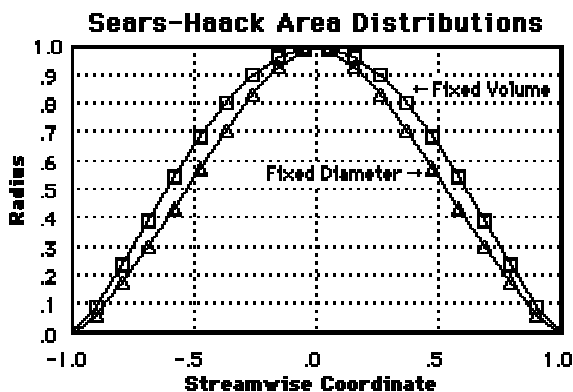
$$\left(\frac{r}{r_0}\right)^2 = \sqrt{1-x^2} - x^2 \ln \frac{1+\sqrt{1-x^2}}{x}$$

$$\left(\frac{r}{r_0}\right)^2 = (1-x^2)^{3/2}$$

$$C_D = 4\pi^2 r_0^2 / l^2$$

$$C_D = \frac{9}{2} \pi^2 r_0^2 / l^2$$

$$\text{or } D = \frac{128 q}{\pi} \frac{\text{Vol}^2}{l^4}$$



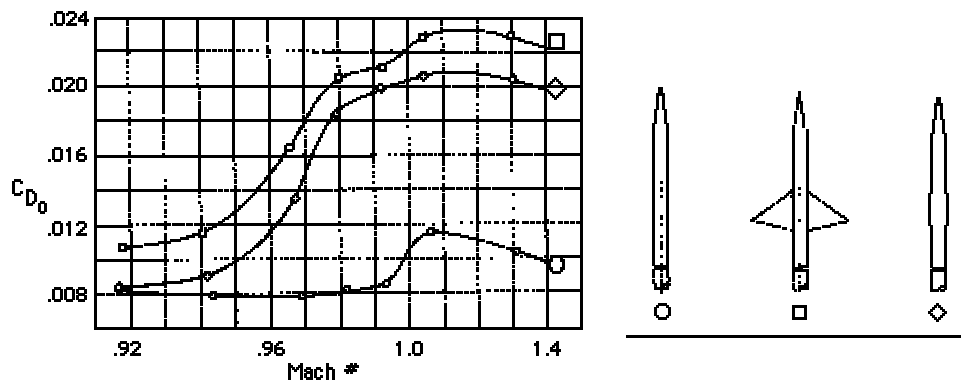
General Shapes

When the body does not have the Sears-Haack shape, the volume dependent wave drag may be computed from linear supersonic potential theory. The result is known as the supersonic area rule. It says that the drag of a slender body of revolution may be computed from its distribution of cross-sectional area according to the expression:

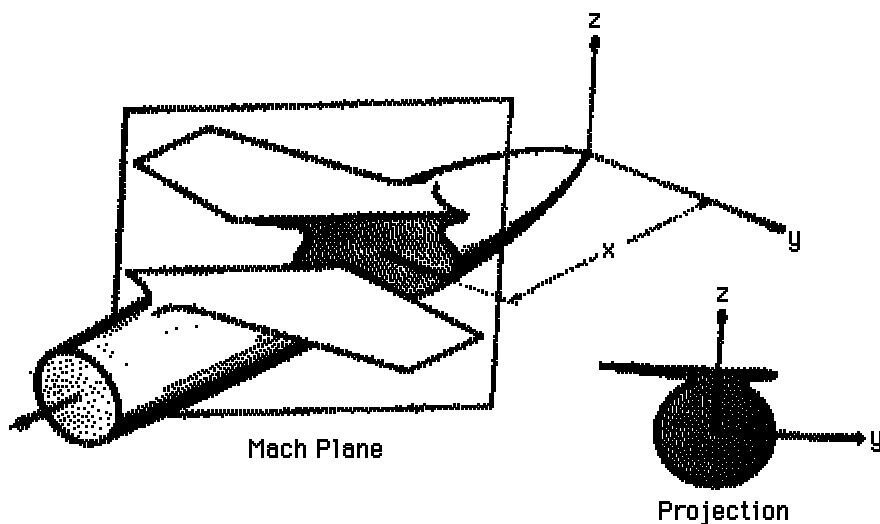
$$D = -\frac{\rho U_\infty^2}{4\pi} \int_0^1 \int_0^1 A''(x_1) A''(x_2) \ln |x_1 - x_2| dx_1 dx_2$$

where A'' is the second derivative of the cross-sectional area with respect to the longitudinal coordinate, x .

For configurations more complicated than bodies of revolution, the drag may be computed with a panel method or other CFD solution. However, there is a simple means of estimating the volume-dependent wave drag of more general bodies. This involves creating an equivalent body of revolution - at Mach 1.0, this body has the same distribution of area over its length as the actual body.



At higher Mach numbers the distribution of area is evaluated with oblique slices through the geometry. A body of revolution with the same distribution of area as that of the oblique cuts through the actual geometry is created and the drag is computed from linear theory.

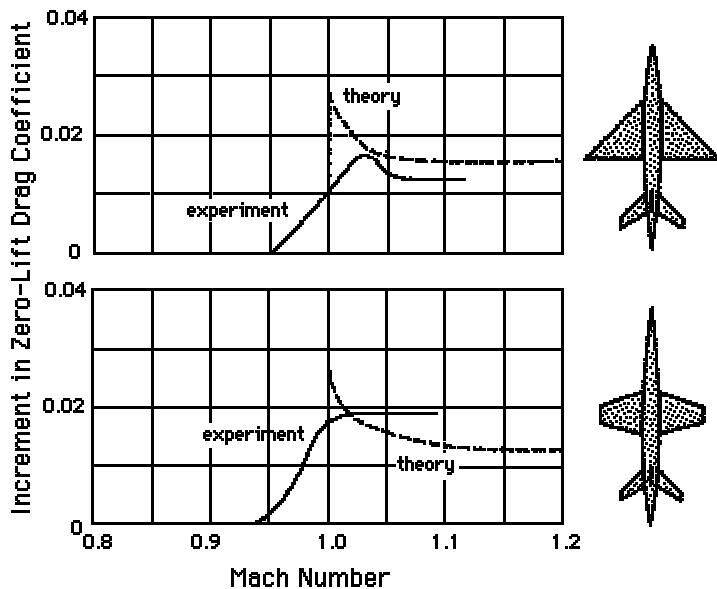


The angle of the plane with respect to the freestream is the Mach angle, $\sin \theta = 1/M$, so at $M=1$, the plane is normal to the flow direction, while at $M = 1.6$ the angle is 38.7° (It is inclined 51.3° with respect to the $M = 1$ case.)

The actual geometry is rotated about its longitudinal axis from 0 to 2π and the drag associated with each equivalent body of revolution is averaged.

$$D = - \frac{\rho U_\infty^2}{8 \pi^2} \int_0^{2\pi} \int_0^1 \int_0^1 A''(x_1, \theta) A''(x_2, \theta) \ln |x_1 - x_2| dx_1 dx_2 d\theta$$

A comparison of actual and estimated drags using this method is shown below.



At the earliest stages of the design process, even this linear method may not be available. For conceptual design, we may add wave drag of the fuselage and the wave drag of the wing with a term for interference that depends strongly on the details of the intersection. For the first estimate in AA241A we simply add the wave drag of the fuselage based on the Sears-Haack results and volume wave drag of the wing with a 15% mark-up for interference and non-optimal volume distributions.

For first estimates of the volume-dependent wave drag of a wing, one may create an equivalent ellipse and use closed-form expressions derived by J.H.B. Smith for the volume-dependent wave drag of an ellipse. For minimum drag with a given volume:

$$C_{D_{ow}} = \frac{t^2}{b^2} \left[\frac{\beta^2 + 2b^2/a^2}{(\beta^2 + b^2/a^2)^{3/2}} \right]$$

where t is the maximum thickness, b is the semi-major axis, and a is the semi-minor axis. β is defined by: $\beta^2 = M^2 - 1$. Note that in the limit of high aspect ratio ($a \rightarrow \text{infinity}$), the result approaches the 2-D result for minimum drag of given thickness:

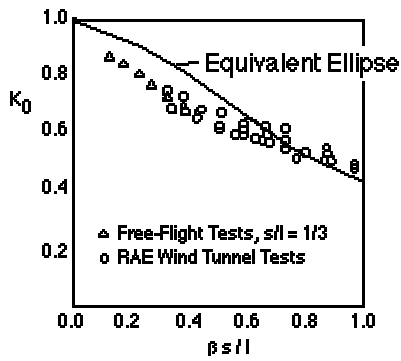
$$C_D = 4 (t/c)^2 / \beta$$

Based on this result, for an ellipse of given area and length the volume drag is:

$$C_D = \frac{128}{\pi^3} \frac{Vol^2}{l^4} K_0 \quad \text{with} \quad K_0 = \frac{2x^2 + 1}{(4x^2 + 1)^{3/2}} \quad \text{and} \quad x = \frac{2}{\pi} \frac{\beta s}{l}$$

where s is the semi-span and l is the overall length.

The figure below shows how this works.



Volume-dependent wave drag for slender wings with the same area distribution. Data from Kuchemann.

Wave Drag Due to Lift

$$\frac{M^2 - 1}{2} \frac{\text{Lift}^2}{q \pi l^2}$$

The expression given for wave drag due to lift:

holds for wings of very low aspect ratio.

A more general expression is derived by R.T. Jones in "Minimum Drag of Airfoils at Supersonic Speeds", J. of Aero Sciences, Dec. 1952.

The combined vortex and wave drag may be written:

$$C_D = \frac{C_L^2}{\pi AR} \sqrt{1 + (M^2 - 1) \left(\frac{\pi AR}{4} \right)^2}$$

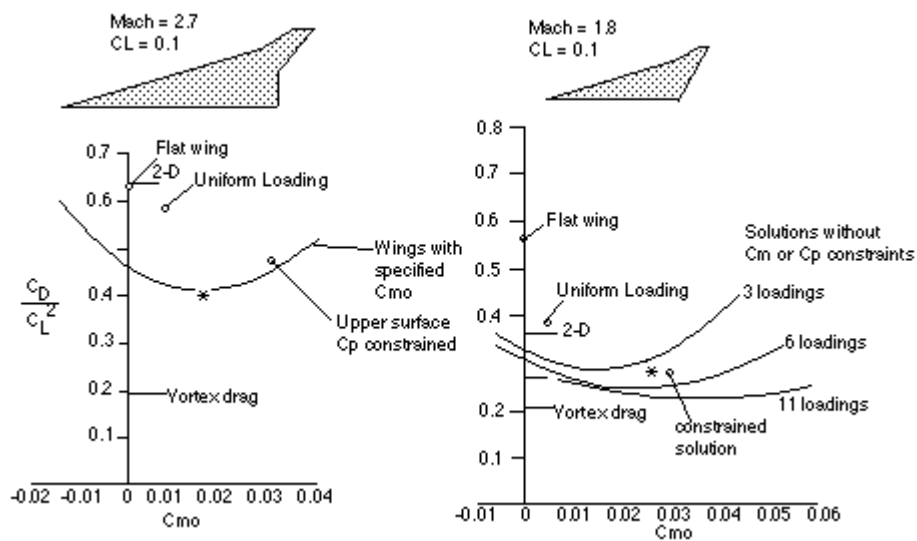
This expression approaches the correct limits for ellipses as $M \rightarrow 1$ and as $AR \rightarrow 0$ or infinity. The assumption here is that the lift distribution is elliptical in all directions, an assumption that is not realized exactly in practice.

Jones also gives an expression for the wave drag due to lift for a yawed ellipse, showing that there is an optimum sweep angle. At $M = 1.4$, a 10:1 yawed ellipse at 55° has less than 1/2 of the wave drag of the ellipse with 0° or 90° of yaw.

When the planform shape is not elliptical, it may be better to form an equivalent ellipse with the same area and length rather than one with the same aspect ratio as the real wing. In this case:

$$C_{D_{w1}} = \frac{\pi l^2}{16 S} C_L^2 \left[\sqrt{1 + (M^2 - 1) \left(\frac{4 S}{\pi l^2} \right)^2} - 1 \right]$$

Here, S is the wing area and l is the overall length. This choice preserves the average wing pressure difference and agrees well with experimental data for well-designed supersonic wings.



Supersonic Drag Due To Lift Computed by Present Method (*) and Boeing Optimization Results